HHS Public Access

Author manuscript

Mol Psychiatry. Author manuscript; available in PMC 2016 January 01.

Published in final edited form as:

Mol Psychiatry. 2015 July ; 20(7): 901–912. doi:10.1038/mp.2014.161.

Durable fear memories require PSD-95

Paul J. Fitzgerald[#,1], **Courtney R. Pinard**[#,1], **Marguerite C. Camp**[#,1], **Michael Feyder**[1], **Anupam Sah**[2], **Hadley Bergstrom**[1], **Carolyn Graybeal**[1], **Yan Liu**[3], **Oliver Schlüter**[5], **Seth G.N. Grant**[4], **Nicolas Singewald**[2], **Weifeng Xu**[3], and **Andrew Holmes**[1,*]

[1]Laboratory of Behavioral and Genomic Neuroscience, National Institute on Alcohol Abuse and Alcoholism, Bethesda, MD, NIH

[2]Department of Pharmacology & Toxicology, University of Innsbruck, Innsbruck, Austria

[3]Department of Brain and Cognitive Science, Massachusetts Institute of Technology, Cambridge, MA, USA

[4]Centre for Clinical Brain Sciences and Centre for Neuroregeneration, The University of Edinburgh, Edinburgh, UK

[5]European Neuroscience Institute, 37077 Gottingen, Germany

Abstract

Traumatic fear memories are highly durable but also dynamic, undergoing repeated reactivation and rehearsal over time. While overly persistent fear memories underlie anxiety disorders such as posttraumatic stress disorder, the key neural and molecular mechanisms underlying fear memory durability remain unclear. Post-synaptic density 95 (PSD-95) is a synaptic protein regulating glutamate receptor anchoring, synaptic stability and certain types of memory. Employing a loss-of-function mutant mouse lacking the guanylate kinase domain of PSD-95 (PSD-95^{GK}), we analyzed the contribution of PSD-95 to fear memory formation and retrieval, and sought to identify the neural basis of PSD-95-mediated memory maintenance using *ex vivo* immediate-early gene mapping, *in vivo* neuronal recordings and viral-mediated knockdown approaches. We show that PSD-95 is dispensable for the formation and expression of recent fear memories, but essential for the formation of precise and flexible fear memories and for the maintenance of memories at remote time points. The failure of PSD-95^{GK} mice to retrieve remote cued fear memories was associated with hypoactivation of the infralimbic cortex (IL) (not anterior cingulate (ACC) or prelimbic cortex), reduced IL single-unit firing and bursting, and attenuated IL gamma and theta oscillations. Adeno-associated PSD-95 virus-mediated knockdown in the IL, not ACC, was sufficient to impair recent fear extinction and remote fear memory, and remodel IL dendritic spines. Collectively, these data identify PSD-95 in the IL as a critical mechanism supporting the durability of fear memories over time. These preclinical findings have implications for developing

[*]*Correspondence to:* Andrew Holmes, PhD, 5625 Fishers Lane Room 2N09, Rockville, MD, USA 20852-9411, Andrew.Holmes@nih.gov, Telephone: 301-402-3519.

[#]Equal contribution

Conflicts of interest and financial disclosures

The authors have no conflicts or competing interests to declare.

novel approaches to treating trauma-based anxiety disorders that target the weakening of overly persistent fear memories.

Introduction

Once formed, fear memories can last a lifetime [1]. However, evidence is accumulating that fear memories are not rigid, but plastic over time and labile following reactivation. Dysregulation of the balance between memory retention and revision, whereby fear memories are long-lasting and inflexible, may contribute to persistent anxiety in disorders such as posttraumatic stress disorder [2, 3]. Indeed, rendering fear memories unstable, and thereby more liable to erasure or reconsolidation, has been proposed as a novel approach to treating anxiety disorders [4]. Currently, however, the critical neural and molecular mechanisms determining fear memory stability and persistence over time are not fully understood [5–9].

Glutamate-mediated signaling and plasticity is critical to various forms of fear learning and memory. By orchestrating protein-protein interactions and the scaffolding of glutamate receptors, PSD-95 plays an integral functional role within the postsynaptic machinery mediating glutamatergic plasticity [10–18]. PSD-95 stabilizes AMPARs at the synapse to promote synaptic function and spine growth, and decreasing PSD-95 leads to loss of synaptic AMPAR content, synaptic weakening, deficient long-term depression, and spine elimination e.g., [12, 16, 17, 19–21] (c.f. [22]). Following fear learning, PSD-95 expression is increased in brain regions such as the amygdala, and these increases are rapidly reversed by the formation of extinction memories that lead to the inhibition of fear [23, 24]. Recent work has also shown that PSD-95 is actively degraded by myocyte enhancer factor 2 (MEF2) [25], and that virally overexpressing MEF2 caused AMPAR endocytosis, reduced synaptic strength and spine density, and impaired fear memory stability [26]. Collectively, these observations implicate PSD-95 as a key contributor to the dynamic regulation of synaptic functions critical for fear memory.

The contribution of PSD-95 to memory has been demonstrated behaviorally by studies showing that PSD-95 deletion or knockdown impairs spatial learning, conditioned taste aversion and simple operant associative learning [27–29]. Conversely, manipulations that lead to an upregulation of PSD-95, including estrogen treatment and insulin substrate-2 deletion, produce improvements in spatial and fear memory [30–32]. Interestingly, there is also emerging evidence that PSD-95 may be crucial to maintaining the stability of certain forms of memories at time points more remote from acquisition. For example, while gene deletion of PSD-95 does not prevent the initial formation and recent expression of ethanol conditioned place preference (CPP), the absence of PSD-95 leads to a loss of CPP within two weeks [33]. Along similar lines, mutant mice with a ligand-binding-deficient knockin mutation of PSD-95 show deficient contextual fear memory expression one week, but not one day, after conditioning [34].

Taken together, the existing evidence provides preliminary support for a role for PSD-95 in various forms of memory, but does not establish the precise role of PSD-95 in fear memory or establish the neural mechanisms that underlie such a role. The present study sought to

clarify these questions by integrating behavioral analysis of a loss-of-function PSD-95 mutant mouse with *ex vivo* immediate-early gene mapping, *in vivo* neuronal recordings and viral-mediated knockdown in specific brain regions. Our results reveal that PSD-95 is dispensable for the formation and expression of recent fear memories, but is essential for the precision and flexibility of recent memories and for their maintenance of remote fear memories. Our data identifying PSD-95 as a critical mechanism in fear memory stability could have implications for developing novel anxiolytic treatments that work to enhance the lability of fear memories.

Materials and Methods

Subjects

PSD-95^{GK} mutant mice were engineered with a disruption of the guanylate kinase (GK) domain of the PSD-95 (*Dlg4*) gene and have been previously reported [33, 35, 36]. In other models, shRNA knockdown or mutation of the PSD-95 GK domain disrupts NMDAR-mediated AMPAR endocytosis and LTD [21]. PSD-95^{GK} were repeatedly backcrossed onto a C57BL/6J background. Analysis of 150 SNP markers at ~15–20 megabase intervals across all autosomal chromosomes confirmed 95% C57BL/6J congenicity (JRS Allele Typing Services, The Jackson Laboratory, Bar Harbor, ME). To avoid potential phenotypic abnormalities resulting from genotypic differences in maternal behavior and early life environment [37], WT and PSD-95^{GK} were littermates generated from HET x HET matings. Mice were bred and maintained at The Jackson Laboratory (Bar Harbor, ME) and shipped to the NIH at 7–9 weeks of age.

Mice were housed with same-sex littermates in a temperature and humidity controlled vivarium under a 12 h light/dark cycle (lights on 0600 h). Testing began at least 1 week after acclimation to the animal facility. Males and females were used. Test-naïve mice were used in each experiment and experimenters remained blind to genotype during testing (subjects were identified by subcutaneously implanted microchips or ear notch). The number of mice tested is given in the figure legends. All procedures were approved by the NIAAA Animal Care and Use Committee and followed the NIH guidelines outlined in ‘Using Animals in Intramural Research.’

General procedures for Pavlovian fear conditioning

Fear conditioning was conducted in a 27 × 27 × 11 cm chamber with transparent walls and a metal rod floor (Context A), as previously described [38]. To provide a distinctive olfactory cue, Context A was cleaned between subjects with a 79.5% water/19.5% ethanol/1% vanilla extract solution. After a 120–180 second acclimation period, the mouse received 3 pairings (60–90 second inter-trial-interval) between a (30-second, 80 dB) white noise cue (conditioned stimulus, CS) and (0.6 mA scrambled) footshock (unconditioned stimulus, US) presented during the last 2 seconds of the tone. Mice remained in the chamber for 120 seconds after the final pairing.

Cued fear memory was tested in a Plexiglas cylinder with black/white-checkered walls and a solid-Plexiglas, opaque floor, cleaned between subjects with a 99% water/1% acetic acid

solution and housed in a different room from training (Context B). After a 180-second acclimation period, the CS was presented continuously for either 180 seconds or via 3 × 30-second presentations (5-sec inter-CS interval). Contextual fear memory was tested via exposure to Context A for 5 min. CS and US presentation was controlled by the Med Associates Freeze Monitor system (Med Associates Incorporated, Georgia, VT). Freezing was defined as the absence of any visible movement except that required for respiration, and was scored at 5-second intervals by an observer blind to genotype. The number of observations scored as freezing were converted to a percentage ([number of freezing observations/total number of observations] × 100) for analysis.

Formation, extinction and precision of fear memory

Recent fear memory: Delay fear was tested using the same procedure described above. Cue fear retrieval was tested 1 day after conditioning, and context fear retrieval the following day (for schematic, see Figure 1a). Trace fear was tested using the same procedure as for delay fear, except for the imposition of a 30-second no-stimulus interval between CS and US presentations during conditioning (interval based on previous studies [39–41]) (for schematic, see Figure 1c).

Fear extinction, retrieval and renewal: Conditioning involved the same delay fear procedure as above. The following day, extinction training was given via 50 × 30-second CS-presentations (5-sec inter-CS interval) in Context B after 180 seconds of context acclimation. The next day, extinction retrieval was tested in Context B via 3 × 30-second CS-presentations (5-second inter-CS interval) after 180 seconds of context acclimation (for schematic, see Figure 1e). Because extinction memories are context dependent, such that extinguished fear will renew when tested in the non-extinguished context [42], fear renewal was also tested (~4 hours after extinction retrieval), via (after 180 sec of acclimation) 3 × 30-second CS-presentations in Context A.

Precision of fear memory: Contextual fear memory discrimination was assessed using previously described procedures [43] (for schematic, see Figure 1g). Conditioning was conducted in Context A (specifications as above) via 3 x US presentations (60–90-second inter-US interval) after 180 seconds of context acclimation. The following day, fear was tested in Context A, Context B (specifications as above) and Context C via 120-second exposure to each context (~4-hour interval between exposures, counterbalancing for the order of context exposure). Context C had a metal grid floor and was the same size and shape as Context A, but had black/white-checkered walls and the same odor as Context B.

Stability of fear memories with time and reactivation

Remote fear memory: Remote cue fear was tested using the same delay fear procedure as above, with the exception that cue retrieval was tested 14 days after conditioning (and there was no contextual fear retrieval test) (for schematic, see Figure 2a). This remote interval was based on previous studies of remote fear memory in mice (e.g., [44]), and evidence of fear memory consolidation across brain systems within 1 week of fear acquisition [45].

In a second experiment, remote contextual fear memory was tested (via 5 min exposure to Context A) 14 days after contextual conditioning (conducted in Context A via 3 x US presentations, 60–90-second inter-US interval, after 180 seconds of context acclimation) (for schematic, see Figure 2c).

A third experiment was conducted to provide a within-subjects comparison of fear retrieval on recent versus remote intervals. Following contextual conditioning, context fear was tested 1 day and again 14 days later using the same procedure as above, with the exception that the recent retrieval test was limited to 120 seconds to minimize extinction (for schematic, see Figure 2e).

Fear reactivation as a function of memory maturity: Mice were given cued fear conditioning and then fear memory was reactivated 1, 3 or 5 days later, in separate groups of mice, via 1 × 30-second CS presentation in Context B, after 180 seconds of context acclimation. Non-reactivated controls received Context B exposure for the equivalent duration (i.e., 210 seconds). Cue retrieval was tested the following day via 3 × 30-second CS-presentations (5-second inter-CS interval) after 180 seconds of context acclimation (for schematic, see Figure S1a).

Fear-related medial prefrontal activation—Activation of cells positive for the plasticity-related immediate-early gene (IEG), Zif268, was examined in subregions of the PFC following memory retrieval, as previously described [46, 47]. Cued fear conditioning and recent and remote retrieval was tested (for schematic, see Figure 3a). Two hours after retrieval, mice were sacrificed via cervical dislocation and rapid decapitation, and brains flash-frozen. Brains were sectioned in the coronal plane at 30 μm thickness on a cryostat (CM1850, Leica Microsystems, Buffalo Grove, IL, USA) and collected on gelatin coated slides.

Sections were post-fixed for 40 minutes in 4% paraformaldehyde and pre-incubated for 30 minutes in normal goat serum. Sections were then incubated with a rabbit anti-Zif268 polyclonal primary antibody (1:5000; sc-189; Santa Cruz Biotechnology, Dallas, TX, USA) and a biotinylated goat anti-rabbit secondary antibody (1:200; Vector Laboratories, Burlingame, CA, USA). An avidin-biotin-horseradish peroxidase procedure (Vectastatin ABC Kit, Vector laboratories, Burlingame, CA, USA) with 3,3′-diaminobenzidine as chromogen (DAB, Sigma, Munich, Germany) was used to visualize Zif268-positive cells. The anatomical localization of Zif268-positive cells was made with reference to a mouse stereotaxic atlas. Cells containing a nuclear brown-black reaction product were considered to be Zif268-positive cells and counted, bilaterally, in a representative tissue area of 0.01 mm^2 with the help of a light microscope (Olympus BX-40, Olympus, Center Valley, PA, USA) equipped with an ocular grid.

Fear-related medial prefrontal neuronal recordings—Implantation of a microelectrode array (Innovative Neurophysiology, Durham, NC, USA) targeting the (right) mPFC (infralimbic cortex (IL) and rostral into medial orbital) was carried out in mice anesthetized with isoflurane and placed in a stereotaxic alignment system (Kopf Instruments, Tujunga, CA, USA). Each array contained 16 × 35 μm-diameter tungsten

microelectrodes arranged into 2 rows of 8 (150 μm spacing between microelectrodes within a row, 200 μm spacing between rows). Rows were positioned lengthwise anterior to posterior (coordinates for center of array, relative to bregma: AP +1.75–1.80, ML +0.35–0.50, DV −2.90). Mice were given at least 1 week of recovery before testing.

Mice were given cued fear conditioning and a within-subjects design was employed to give the same mice the recent and remote retrieval tests. Additionally, to measure basal firing and single-unit responses to the CS prior to fear conditioning, mice were tested and recorded in a unique context 1 day prior to conditioning, using the same procedure as for conditioning, but with no US presentation. Recordings were made using a Multichannel Acquisition Processor (Plexon Inc, Dallas, TX, USA) as previously described [48–51]. Extracellular waveforms exceeding a set voltage threshold were digitized at 40 kHz and stored in a PC. Waveforms were manually sorted using principal component analysis of spike clusters and visual inspection of waveforms and inter-spike intervals.

Neuronal activity was time-stamped to CS onset, and spike and timestamp information integrated and analyzed using NeuroExplorer (NEX Technologies, Littleton, MA, USA). Activity 2 seconds after CS onset was Z-score normalized to activity during a 1 second pre-CS baseline and presented in 100 millisecond perievent histograms. CS-related single-units were defined as a unit with an increase in firing during the first 100 milliseconds of CS-onset that was >3 standard deviations from the unit's pre-CS baseline firing. CS-related burst firing was defined as 3 or more consecutive spikes with an interspike interval of <25 milliseconds between the first 2 spikes and <50 milliseconds between subsequent spikes, and was expressed as the percentage of all CS-related firing [48, 51, 52].

Local field potential (LFP) waveforms were sampled at 1 kHz, pre-amplified at 1000× and low-pass filtered at 250 Hz. The NeuroExplorer perievent spectrogram function was used to calculate power density values for each LFP, with PSD values expressed as power per frequency, binned into 0.02 Hz bins and smoothed using a post-processing filter width of 5 bins to determine the average power density within the theta (4.5–8 Hz) and gamma (30–70 Hz) ranges. The NeuroExplorer perievent spectrogram function (waveforms high-pass filtered at 4 Hz, frequency binned into 0.30 Hz bins for theta activity and into 0.15 Hz bins for gamma activity) was used to plot representative spectrograms of the power density of LFP activity.

At the completion of testing, array placement was verified by passing 100 μA current through the electrodes for 20 seconds using a current stimulator (S48 Square Pulse Stimulator, Grass Technologies, West Warwick, RI, USA) to make electrolytic lesions. Brains were removed and 50 μm coronal sections cut with a vibratome (Classic 1000 model, Vibratome, Bannockburn, IL, USA) and stained with cresyl violet. Placements were estimated with the aid of an Olympus BX41 microscope (Olympus, Center Valley, PA, USA) and referenced to a mouse stereotaxic atlas (for placements, see Figure S2a).

Medial prefrontal PSD-95 knockdown

Adeno-associated virus generation: The PSD-95 knockdown adeno-associated virus (pAAV-H1-sh95-CAG-GFP) was modified from the pAAV-CAG-GFP virus, which served

as a control [53]. Briefly, the EcoRI site between eGFP and WPRE in pAAV-CAG-GFP was destroyed, and EcoRI and BstBI sites were introduced upstream of the NdeI site (pAAV-EB-CAG-GFP). An H1 promoter-driven shRNA expression cassette targeting the mouse PSD-95 sequence (TCACG ATCATCGCTCAGTATA) [15] was introduced at the EcoRI/BstBI site. rAAVs were purified using a 1 ml heparin column and concentrated using the Amicon 100kDa cutoff columns [54–56].

One Tx175 flask of 80–90 % confluent HEK293 cells was transfected with the expression plasmid together with plasmids pDp1 (serotype 1) and pDp2 (serotype 2) at the amount of 20, 10 and 10 μg each. Sixty hours after transfection, HEK293 cells were washed once with phosphate-buffered saline (PBS), collected into 15 ml falcon tubes with 5 ml cold PBS supplemented with 5 mM EDTA, and pelleted by centrifugation at 800 × g for 5 minutes. The pellet was washed with PBS, and re-suspended in 0.75 ml of the lysis buffer (150 mM NaCl, 50 mM Tris; pH8.4). The lysate was frozen-thawed 3 times at −70 °C with dry ice/ethanol and 37°C with water bath. Benzonase was supplemented to the lysate at a final concentration of 50 U/ml. The cell lysate was then incubated at 37 °C for 60 minutes and centrifuged at 3,000 × g for 15 minutes at 4 °C. The supernatant was collected with a syringe and filtered through a 32 mm 0.45 μm Acrodisc syringe filter and loaded to a pre-equilibrated heparin column (pre-equilibrated with PBS-MK, PBS + 1mM $MgCl_2$, 2.5 mM KCl, pH 7.2) at a rate of 1 ml per minute. The column was washed with PBS-MK, and the virus was eluted with 5 volumes of PBS-MK + 0.5 M NaCl. The virus solution was washed and concentrated with PBS at least twice in a 15 ml Amicon 100kDa column with centrifugation of 5,000 × g at 4°C. The final viral suspension was aliquoted and stored at −80 °C. The genomic copy numbers of the 2 viruses were ~1×10^9 copies per ml, tested with qPCR with GFP primers.

The efficacy of the virus was confirmed in vitro by quantifying PSD-95 protein loss using Western blot, and by visualizing green fluorescent protein (GFP) expression in infected brain tissue, *ex vivo* (Figure 5a–c). For Western blot, dissociated mouse cultures were prepared using standard methods [57]. Neurons were infected with rAAV viruses at DIV7 and cell lysates were collected at DIV 17 for western blot analysis with PSD-95 (Thermo Fisher Scientific, Rockville, MD, USA, catalogue #MA1-046) and β-actin (Sigma Aldrich, St Louis, MO, USA, catalogue #A2228) antibodies.

Behavioral testing: For behavioral experiments, virus was infused into the brain via stereotaxic surgery (as described above for microelectrode implantation) using a Hamilton syringe with a 33 gauge needle (Hamilton, Reno, NV, USA). A total volume of 0.25 μmole of the virus was infused at a rate of 0.02 μmole per minute. Virus was bilaterally infused into either the IL (coordinates relative to bregma: AP +1.8, ML +0.25, DV −3.0) or the ACC (coordinates relative to Bregma: AP +2.1, ML +0.25, DV −2.0). The needle was left in place for 5 minutes to allow for diffusion and the scalp was cleaned and sutured. Mice were left undisturbed for 2 weeks to allow for virus expression. Mice were tested for cued fear conditioning and subsequent recent and remote retrieval (for schematic, see Figure 5d). In a separate experiment, mice were tested for fear extinction (for schematic, see Figure 5f).

At the completion of testing, mice were terminally overdosed with ketamine/xylazine and transcardially perfused with phosphate buffered saline, then 4% paraformaldehyde (PFA). After suspension in 4% PFA overnight and then 4°C 0.1M phosphate buffer for 1–2 days, 50 μm coronal sections were cut with a vibratome (Classic 1000 model, Vibratome, Bannockburn, IL, USA) and coverslipped with Vectashield HardSet mounting medium and DAPI (Vector Laboratories, Inc., Burlingame, CA, USA). Virus location was estimated by visualizing fluorescence with the aid of an Olympus BX41 microscope (Olympus, Center Valley, PA, USA) (for estimates, see Figure S2a). Four out of 33 mice were discarded because of poor or misplaced virus expression.

Dendritic spine analysis: Virally infected dendritic segments on IL pyramidal neurons were identified under a 10X/1.2 N.A. objective (Zeiss Model LSM 700, Carl Zeiss Microscopy, Thornwood, NY, USA). Segments that met all of the following criteria were selected for analyses: 1) were >150 μm from the soma, 2) showed clear spine protrusions, 3) were not obscured by other dendrites, and 4) were parallel or near parallel with the coronal plane of the section. All confocal stacks comprised ±5 μm above and below the extent of the dendritic segment. Segments were imaged under a 63X/1.4 N.A. oil-immersion objective, using voxel dimensions 0.1 × 0.1 × 0.1 μm^3 and 2.5 X zoom at a resolution of 512 × 512 pixels. Z series were obtained by imaging serial confocal planes at 0.20 μm intervals. Settings for pinhole size (1 airy disc) and gain (600) were optimized initially and remained constant throughout imaging to ensure images were digitized under consistent illumination. These parameters resulted in dendritic segments ~30–80 μm in length. Data were obtained from 3–8 segments per neuron.

Spines were designated manually from digital confocal image stacks using NeuronStudio software [58]. Spine density was calculated as the number of spines divided by dendritic segment length. Spine head width was defined as the maximum diameter of the spine head. For analysis of PSD-95 knockdown in IL neurons, data were additionally segregated into narrow and wide spines using a median split based on head width. As in previous analyses [59], spines > 4.0 μm in length were not included in the analysis.

Statistical analysis: Effects of genotype x conditioned-to-retrieval interval, genotype x recording timebin and genotype x CS-onset were analyzed via 2-factor analysis of variance (ANOVA) followed by Fisher's Least Significant Difference (LSD) post hoc tests. Effects of genotype on CS-related units (as a percentage of total recorded per genotype and task-phase) were analyzed using the Chi-square test. Effects of extinction test-phase and context-type were analyzed via repeated measures ANOVA followed by Fisher's LSD post hoc tests. The effect of genotype and viral knockdown on levels of freezing, the number of Zif268-labeled cells and spine density/morphology was analyzed using Student's *t*-tests. The threshold for statistical significance was set at $P<.05$.

Results

Formation and retrieval of recent fear memories

We began by testing the contribution of PSD-95 to fear memory formation and the expression of these memories within the first few days of learning. To this end, mice were

first tested for the ability to form fear memories for cues and contexts, using delay and trace versions of conditioning. Following multi-trial fear conditioning, freezing was no different between genotypes during pre-conditioning baseline or the final conditioning-CS presentation (Table S1). Genotypes also showed equivalent levels of freezing during cue retrieval, measured 1 day after multi-trial delay cued conditioning, and similar freezing during context retrieval, tested 2 days after conditioning (Figure 1b). To confirm that a subtle memory deficit in PSD-95^{GK} was not being masked by overtraining in the multi-trial procedure, a separate cohort of mice underwent one-trial conditioning using a single (0.8 mA) US, as previously described [40]. Genotypes did not differ in freezing during cue (WT=79.6±4.0, MUT=70.8±7.7, n=6=9) or context (WT=32.8±10.3%, MUT=22.5±6.6, n=6–9) retrieval following one-trial conditioning. Finally, in a cohort given trace fear conditioning in which there was a longer interval between cue and shock, genotypes did not differ in freezing during pre-conditioning baseline, but PSD-95^{GK} mice froze more than WT controls to the final CS presentation ($t(16)=3.58$, $P<.01$) (Table S1). Genotypes showed similar freezing during cue fear retrieval, but the PSD-95^{GK} mice froze less than WT controls during context retrieval ($t=2.20$, $df=16$, $P<.05$) (Figure 1d). Thus, PSD-95^{GK} mice failed to fully form an association with a fear-associated context when the context was experienced as a background stimulus to temporally discontiguous cued fear learning.

Overall, the results of these initial experiments demonstrate that loss of PSD-95 has minimal effects on the ability to form and express most recently acquired fear memories. However, impaired trace context fear in the PSD-95^{GK} mice hints at certain fear memory deficits in the mutants, potentially reflecting abnormalities when structures mediating trace fear, such as the hippocampus and mPFC [60], are more strongly taxed.

Extinction and precision of recent fear memories

To further probe the nature of the fear memories formed in the absence of PSD-95, we examined fear extinction and memory precision. We first asked whether, once a fear memory has been generated, loss of PSD-95 affects the ability to extinguish it. During multi-trial cued fear conditioning, PSD-95^{GK} mice froze slightly more than WT controls during baseline ($t(26)=2.81$, $P<.01$) and the final CS presentation ($t(26)=2.52$, $P<.05$) (Table S1). However, genotypes did not differ in freezing during recent fear memory retrieval, as indicated from freezing on the first trial-block of extinction training. By contrast, while WT controls decreased freezing from the first to last extinction trial-block, PSD-95^{GK} mice showed no reduction in freezing across trial-blocks (genotype x trial-block interaction: $F1,26=12.76$, $P<.01$) (Figure 1f). Moreover, WT controls froze less during extinction retrieval, relative to the first trial-block of extinction training, indicating successful extinction memory retrieval ($t(13)=4.56$, $P<.01$), whereas PSD-95^{GK} mice did not show a reduction (Figure 1f). Finally, WT controls froze more during the fear renewal test as compared to extinction retrieval ($t(13)=6.68$, $P<.01$), but PSD-95^{GK} mice did not (Figure 1f).

These findings indicate that recent fear memories formed in the absence of PSD-95 are highly resistant to extinction. In light of the recent finding that the cell surface expression of PSD-95 and AMPARs is decreased with extinction [23], these data suggest that dynamic

changes in PSD-95 may be a molecular signal for extinction. Another, not necessarily exclusive, possibility is that the PSD-95^{GK} mice failed to retrieve a sufficiently accurate representation of the original CS-shock association to permit effective reappraisal of the association with extinction. To examine the precision of fear memory in the PSD-95^{GK} mice, we assessed the retrieval of a contextual fear memory by conditioning mice to Context A and then testing for fear to either that context or 2 dissimilar contexts (B and C). WT controls froze more to Context A than Context B or C ($F_{2,24}=8.91$, $P<.01$). By contrast, PSD-95^{GK} mice froze at the same level to all 3 contexts (Figure 1h). This indicates a failure of discriminative contextual fear memory in the mutants. Whether discrimination of cued fear memories is also impaired remains unclear and will be an interesting question for future studies.

Thus, though PSD-95 is not necessary for the formation and recent retrieval of fear memories, the fear memories that are generated without PSD-95 are imprecise, as well as resistant to extinction. In other words, when PSD-95 is deleted, alternate mechanisms can support the formation of fear memories, but the resultant memories are rigid and qualitatively inferior to those produced in the presence of PSD-95.

Retrieval of remote fear memories

Our next set of experiments asked whether the type of fear memories formed in the absence of PSD-95 remained robust over time. In our first experiment, genotypes froze at similar levels during pre-conditioning baseline and, as in earlier experiments, PSD-95^{GK} mice froze more than WT controls to the final CS presentation of multi-trial cued fear conditioning ($t(15)=2.82$, $P<.01$) (Table S1). On a remote retrieval test two weeks after conditioning, PSD-95^{GK} mice showed markedly less freezing than WT controls ($t(15)=5.19$, $P<.01$) (Figure 2b). This finding of reduced remote-freezing was replicated in a second cohort of PSD-95^{GK} mice tested under the same conditions ($t(11)=6.02$, $P<.01$, n=6–7, data not shown).

Deficient retrieval of remote memories in the PSD-95^{GK} mice extended to contextual fear memory. Following multi-trial context conditioning, PSD-95^{GK} mice froze less than WT controls during a remote retrieval test two weeks after conditioning ($t(17)=3.21$, $P<.01$) (Figure 2d). Another experiment using a within-subjects design demonstrated the time-dependent loss of memory in the same PSD-95^{GK} mice - genotypes froze at similar levels during recent retrieval, but the PSD-95^{GK} mice froze less than WT controls when retested 2 weeks later (genotype x day interaction: $F_{1,14}=10.21$, $P<.01$) (Figure 2f).

These observations confirm and extend earlier evidence that PSD-95 deficiency impairs remote CPP and contextual fear [33, 34] by showing that PSD-95 is essential for the retention of fear memories at remote time points.

Stability of reactivated fear memories within one week of acquisition

If fear memories formed in the absence of PSD-95 are quicker to decay with time, they may also become increasingly fragile as they age. We tested for this by reactivating memories at progressively longer intervals (1, 3 or 5 days) after conditioning, in separate groups of mice,

and then probing memory the following day (Figure S1a). During multi-trial cued conditioning, genotypes froze at similar levels during baseline and PSD-95^{GK} mice froze more than WT controls to the final CS presentation ($t(92)=2.38$, $P<.05$) (Table S1). On the retrieval tests, freezing was affected by genotype and memory reactivation in a time dependent manner (genotype x day interaction: $F2,82=3.72$, $P<.05$). Specifically, genotypes froze at similar levels during retrieval 2 days after conditioning, irrespective of whether memory had been reactivated the day before. Conversely, PSD-95^{GK} mice froze less than WT controls when tested 4 days after conditioning, but only if memory had been reactivated the day before (Figure S1b). Moreover, PSD-95^{GK} mice tested 6 days after conditioning froze less than WT controls regardless of prior reactivation, though freezing in the mutants was reduced to a greater extent if memory had been reactivated the previous day (Figure S1b).

These preliminary data reveal that by the end of the first week after acquisition, loss of PSD-95 renders fear memories vulnerable to disruption by reactivation. This effect is particularly striking given fear memories typically become more, not less, resistant to destabilization as they age [61, 62].

Infralimbic recruitment by remote fear memories

Our next objective was to localize the neural basis of the age-dependent fear memory impairment caused by loss of PSD-95. Earlier work has shown that retrieval of multiple forms of remote memory, including spatial learning, cocaine reinstatement, conditioned taste aversion, trace-eye blink conditioning, and contextual fear, becomes dependent on sensory [63] and prefrontal cortical regions [61, 64–76]. Protein synthesis in the PFC is also necessary for remote contextual fear memory reconsolidation [61]. Moreover, a phenotype of impaired remote fear memory retrieval (e.g., in αCaMKII deficient mice) analogous to that currently observed in the PSD-95^{GK} mice, is associated with deficient activation of areas of the PFC [77]. On the basis of these various observations, we examined recruitment of the PFC following retrieval of recent and remote fear memories by quantifying expression of the plasticity-related immediate-early gene (IEG), Zif268, in the IL, prelimbic cortex (PL) and Cg1 subregion of the ACC [77].

Genotypes froze at similar levels during pre-conditioning baseline and PSD-95^{GK} mice froze more than WT controls to the final CS presentation ($t(34)=2.32$, $P<.05$) (Table S1). As expected, PSD-95^{GK} mice froze less than WT controls during remote, but not recent, cue fear retrieval (genotype × day interaction: $F1,32=25.18$, $P<.01$) (Figure 3b). IEG analysis of prefrontal regions (Figure 3c) found no change in the number of Zif268-positive cells in either the PL or ACC (Figure 3d), irrespective of memory age or genotype. However, WT mice exhibited an elevated number of Zif268-positive cells in the IL after remote, as compared to recent retrieval ($t(14)=2.30$, $P<.05$), while the number of cells did not increase in the PSD-95^{GK} mice (Figure 3e,f). Thus, consistent with a model whereby cortical regions become critical to the expression of fear memories as they age [64, 78], these data identify a failure of IL recruitment as one possible neural locus for the impaired remote fear memory in the PSD-95^{GK} mice. The IL is particularly well positioned to mediate fear via rich, PSD-95-positive projections to the amygdala [79] although interestingly, the IL-specific

involvement found here reflects a more restricted pattern of PFC activation with remote fear retrieval of a discrete cue than that typically seen with remote fear retrieval of contextual fear, which encompasses IL, PL and ACC [77].

Dendritic spines are posited to be physical sites of memory storage and the enlargement of spines is coupled to the functional potentiation of synapses [80]. In turn, spine morphology is tightly regulated by PSD-95; for example, PSD-95 increases and persists in enlarged spine and those spines that are rich in PSD-95 are highly stable over time, while knockdown of the guanylate kinase domain of PSD-95 disrupts spine growth [81–83]. Moreover, previous studies have shown that successful remote context fear memory associates with, and may require, spine growth in subregions of the PFC (in this case, the ACC) [84, 85]. We therefore asked whether memory-associated IL hypofunction was associated with dendritic spine abnormalities by quantifying the spine density and morphology of GFP-labelled IL pyramidal neuronal dendrites in behaviorally-naïve PSD-95^{GK} mice and WT controls (Figure 3g). This analysis found that PSD-95^{GK} mice had marginally lower IL dendritic spine density (t(17=1.88, *P*<.077) and significantly narrower head width (t(17=2.99, *P*<.01), as compared to WT controls (Figure 3h). These data reveal a spine morphology correlate of the fear memories caused by loss of PSD-95. The absence of PSD-95 in the IL may disrupt the spine remodeling and associated synaptic strengthening necessary to support the maintenance of a remote memory and other IL-dependent behaviors, including extinction memory formation.

Infralimbic encoding of recent and remote fear memories

While our *ex vivo* IEG and spine morphology results implicate the IL in deficient remote fear retrieval in the PSD-95^{GK} mice, these approaches have limited scope to establish a close functional and temporal link between IL neuronal activity and memory retrieval. Therefore, we next performed *in vivo* recordings of CS-evoked IL single-unit firing as mice retrieved recent and remote fear memories.

Genotypes froze at similar levels during pre-conditioning baseline and PSD-95^{GK} mice froze more than WT controls to the final CS presentation (t(10)=2.24, *P*<.05) (Table S1). PSD-95^{GK} mice also froze more than WT controls during recent retrieval in this experiment (WT=59±2%, PSD-95^{GK}=72±5, t(10)=2.36, *P*<.05), possibly due to sensitivity to the more stressful recording test conditions. Nonetheless, PSD-95^{GK} mice showed lower freezing than WT controls during the remote test (WT=64±4%, PSD-95^{GK}=43±4, t(10)=3.66, *P*<.01). Our recording data showed that genotypes did not differ in baseline unit firing (i.e., pre-CS data, averaged across test phases) (Figure S2b). In addition, recordings made during pre-conditioning, showed that the CS produced a slight but significant increase in Z-scored unit firing (time: F29,4350=2.93, *P*<.01) that did not differ between genotypes (Figure S2c).

Following conditioning, unit firing changed after CS-onset in a genotype-dependent manner during recent (time x genotype interaction: F29,4466=1.84, *P*=.05) and remote (time × genotype interaction: F29,4650=1.45, *P*=.055) retrieval (Figure 4a). Specifically, IL neurons increased firing during the 100-millisecond post-CS interval in WT controls, but not PSD-95^{GK} mice, on both retrieval tests (Figure 4a **insets**). Further confirming genotype differences in CS-related IL firing, the number of ‘phasic IL units’ that fired to the CS at >3

standard deviations over pre-CS baseline were higher in WT mice than PSD-95^{GK} mice during recent ($\chi(1)=9.30$, $P<.01$) and remote ($\chi(1)=14.89$, $P<.01$) retrieval (Figure 4b). In addition, correlating firing and behavior during remote retrieval revealed that high IL unit firing was associated with higher freezing ($r= +0.67$, $P<.05$) (Figure 4c). Finally, we found that the bursting of IL unit firing was increased over pre-CS baseline in both genotypes during recent retrieval (CS: $F1,156=20.94$, $P<.01$), but was increased in WT mice and not in PSD-95^{GK} mice during remote retrieval (CS × genotype interaction: $F1,163=5.88$, $P<.05$) (Figure 4d). Attenuated IL burst firing in the mutants is consistent with earlier work showing that low bursting predicts deficient retrieval of other IL-dependent memory fear memories (e.g., extinction) [48, 52, 86, 87].

In addition to these marked differences in single-unit activity, analysis of local field potentials (LFP) revealed lower gamma (genotype: $F1,20=81.96$, $P<.01$) and theta ($F1,20=17.74$, $P<.01$, test: $F1,20=7.45$, $P<.05$) oscillations in the PSD-95^{GK} mice relative to WT controls, during recent and remote retrieval (Figure 4e,f). The loss of gamma and theta power in the mutant IL is generally consistent with prior studies showing that low power at these frequencies predicts loss of memory retrieval. For example, the strength of gamma and theta oscillations in the human frontal cortex during learning correlates with the strength of subsequent episodic memory retrieval [88]. Similarly, increased gamma power in the rodent auditory cortex, PL or BLA is associated with relatively strong fear learning and the maintenance of high fear after extinction [51, 89, 90]. Low, extinction-induced, fear also correlates with reduced theta oscillations between the mPFC and BLA [91], though a weak or inverse relationship between mPFC (primarily PL) theta power and freezing is seen in some studies [51, 92].

Together, these electrophysiological findings provide compelling, *in vivo* evidence of deficient IL recruitment during fear memory retrieval in the PSD-95^{GK} mice. Notably, the loss of IL neuronal firing and LFP power was evident during the recent and remote memory tests even though only remote retrieval was impaired. Indeed, WT controls showed strong firing during both tests despite our IEG data showing greater region-wide IL recruitment with remote retrieval. Together, these data suggest that while lesion studies show PFC regions are dispensable for recent memory retrieval [64], the retrieval of recent cued memories does actively engage IL neurons. This is consistent with models in which PFC neurons are recruited early and ‘tagged’ during memory formation, but only acquire a demonstrable functional role with time, as memories are replayed and cortico-hippocampal networks are reorganized [78, 93]. Of note, this early tagging process is known to be dependent on PSD-95 related mechanisms including AMPAR and NMDAR signaling [93]. These data raise the possibility that impaired memory persistence caused by loss of PSD-95 may partly originate in an inability to effectively tag fear memories in the IL during formation.

Infralimbic PSD-95 mediation of recent fear extinction and remote fear memory

Our findings thus far provide convergent, correlative evidence that loss of PSD-95 in the IL destabilizes remote cued fear memories, but do not constitute causal support for this. Therefore, our final step was to test whether PSD-95 loss specifically within the IL affected

fear memory retrieval by engineering a PSD-95 knockdown (KD) virus and infusing it into the IL of C57BL/6J mice (Figure 5a,b).

We found that in mice infused 2 weeks prior to multi-trial cued conditioning (Figure 5c), freezing did not differ between PSD-95 KD mice and GFP-virus controls during pre-conditioning baseline or the final CS presentation (Table S1). The groups also showed similar freezing during recent fear memory retrieval. By contrast, PSD-95 KD mice froze less than GFP controls during remote fear memory retrieval ($t(27)=2.22$, $P<.05$) (Figure 5d). In a separate cohort of mice tested for fear extinction after multi-trial cued conditioning, groups did not differ in freezing during baseline or the final CS presentation of conditioning (Table S1), or the first trial-block of extinction training (Figure 5g). However, PSD-95 KD mice showed a significant, but lesser reduction in freezing across trial-blocks than GFP-virus controls (virus: $F1,14=15.80$, $P<.01$; trial-block: $F1,14=63.98$, $P<.01$; genotype x trial-block interaction: $F1,14=4.87$, $P=.053$) (Figure 5g). In addition, while GFP-virus controls froze less during extinction retrieval than in the first trial-block of extinction training ($t(8)=5.82$, $P<.01$), PSD-95 KD mice failed to reduce freezing (Figure 5g). GFP-virus controls froze more during the fear renewal test as compared to extinction retrieval ($t(8)=9.81$, $P<.01$) (Figure 5g). These data confirm that loss of PSD-95 within the IL is sufficient to impair retrieval of remote but not recent fear memories, as well as recent fear extinction, and thereby establish a causal link between IL-PSD-95 and these behaviors.

We also found that, analogous to our findings in PSD-95^{GK} mice, the behavioral impairments in IL PSD-95 KD mice were associated with abnormal morphology of dendritic spines in virally infected IL pyramidal neurons (Figure 5h). Overall spine density and head width was not significantly affected by PSD-95 KD, indicating a more subtle effect of the viral knockdown than the constitutive gene mutation - which caused an overall reduction in spine head width in the IL. However, a median split into relatively wide and narrow spines (Figure 5i), revealed that the head width of wider spines was significantly less in PSD-95 KD mice, relative to GFP controls ($t(33)=2.23$, $P<.05$) (Figure 5j). Consistent with a selective narrowing of head size rather than an overall loss of wide spines, the density of wide or narrow spines was not different between groups, (Figure 5k). These data provide further evidence of a functional link between PSD-95 regulation of IL dendritic spine morphology and IL-mediated extinction and remote cued memory.

While the current findings clearly implicate PSD-95 in IL neurons in the behaviors found to be disrupted by loss of PSD-95, they do not fully exclude a role for PSD-95 in other brain regions. Of note, the dorsal hippocampus, basolateral amygdala and ACC are all known to be important for remote context fear under certain conditions [77, 94, 95]. In this context, the magnitude of recent extinction and remote memory impairments produced by IL KD was less than that caused by the constitutive loss-of-function in PSD-95^{GK} mice. This could either reflect incomplete viral-induced deletion of PSD-95 in IL, or the extant capacity for PSD-95 in other regions, such as the ACC and hippocampus, to partially support behavior. We did find, however, that when the PSD-95 KD virus was infused into the ACC prior to conditioning, freezing was unaltered on the remote (or recent) test (Figure 5e). Therefore, in agreement with our negative ACC IEG data, this region, unlike the IL, does not appear to be critical to the retrieval of remote cued fear memories. Notwithstanding, it would be

premature to rule out a contribution of PSD-95 in other brain regions to this behavior, and further work will be needed to explore this more comprehensively.

Discussion

Despite its known role as a key postsynaptic molecule, essential to various forms of learning, the current study found that various types of Pavlovian fear memory could be acquired and expressed in the absence of functional PSD-95. However, the fear memories that were formed were imprecise and inflexible and, at more remote time points, were readily disrupted with reactivation and eventually lost. Loss of remote fear memory in PSD-95^{GK} mice was associated with decreased regional IL recruitment, as well as reduced IL neuronal firing and bursting. Establishing a causal relationship between IL PSD-95 and fear durability, virus-mediated knockdown of PSD-95 in the IL was sufficient to alter IL dendritic spine morphology and disrupt recent fear extinction and remote fear memory. Collectively, these data reveal PSD-95 as a critical mechanism underlying the maintenance of fear memories over time, and localize at least some of this function to the IL. These findings further our understanding of the neural and molecular basis of disorders in which fear memories are overly persistent, and raise the prospect of targeting PSD-95 as a novel therapeutic approach to weaken traumatic memories.

Supplementary Material

Refer to Web version on PubMed Central for supplementary material.

Acknowledgements

We are very grateful to Katie Kaugars for technical assistance. Research supported by NIAAA Intramural Research Program (A.H.), the Austrian Science Fund (FWF): P22931-B18 and Sonderforschungsbereich (SFB F4410-B19) (N.S), NIH MH080310 (W.X.), and a Simons Seed Grant at MIT (W.X.).

References

1. Gale GD, Anagnostaras SG, Godsil BP, Mitchell S, Nozawa T, Sage JR, et al. Role of the basolateral amygdala in the storage of fear memories across the adult lifetime of rats. J Neurosci. 2004; 24(15):3810–3815. [PubMed: 15084662]
2. Parsons RG, Ressler KJ. Implications of memory modulation for post-traumatic stress and fear disorders. Nat Neurosci. 2013; 16(2):146–153. [PubMed: 23354388]
3. Griebel G, Holmes A. 50 years of hurdles and hope in anxiolytic drug discovery. Nat Rev Drug Discov. 2013; 12(9):667–687. [PubMed: 23989795]
4. Auber A, Tedesco V, Jones CE, Monfils MH, Chiamulera C. Post-retrieval extinction as reconsolidation interference: methodological issues or boundary conditions? Psychopharmacology (Berl). 2013; 226(4):631–647. [PubMed: 23404065]
5. Besnard A, Caboche J, Laroche S. Reconsolidation of memory: a decade of debate. Prog Neurobiol. 2012; 99(1):61–80. [PubMed: 22877586]
6. Tronson NC, Taylor JR. Molecular mechanisms of memory reconsolidation. Nat Rev Neurosci. 2007; 8(4):262–275. [PubMed: 17342174]
7. Johansen JP, Cain CK, Ostroff LE, LeDoux JE. Molecular mechanisms of fear learning and memory. Cell. 2011; 147(3):509–524. [PubMed: 22036561]
8. Dudai Y. The restless engram: consolidations never end. Annu Rev Neurosci. 2012; 35:227–247. [PubMed: 22443508]

9. Graff J, Joseph NF, Horn ME, Samiei A, Meng J, Seo J, et al. Epigenetic priming of memory updating during reconsolidation to attenuate remote fear memories. Cell. 2014; 156(1–2):261–276. [PubMed: 24439381]
10. Fernandez E, Collins MO, Uren RT, Kopanitsa MV, Komiyama NH, Croning MD, et al. Targeted tandem affinity purification of PSD-95 recovers core postsynaptic complexes and schizophrenia susceptibility proteins. Mol Syst Biol. 2009; 5:269. [PubMed: 19455133]
11. Kim E, Sheng M. PDZ domain proteins of synapses. Nat Rev Neurosci. 2004; 5(10):771–781. [PubMed: 15378037]
12. Nelson CD, Kim MJ, Hsin H, Chen Y, Sheng M. Phosphorylation of Threonine-19 of PSD-95 by GSK-3beta is Required for PSD-95 Mobilization and Long-Term Depression. J Neurosci. 2013; 33(29):12122–12135. [PubMed: 23864697]
13. Chen X, Nelson CD, Li X, Winters CA, Azzam R, Sousa AA, et al. PSD-95 is required to sustain the molecular organization of the postsynaptic density. J Neurosci. 2011; 31(17):6329–6338. [PubMed: 21525273]
14. El-Husseini AE, Schnell E, Chetkovich DM, Nicoll RA, Bredt DS. PSD-95 involvement in maturation of excitatory synapses. Science. 2000; 290(5495):1364–1368. [PubMed: 11082065]
15. Elias GM, Funke L, Stein V, Grant SG, Bredt DS, Nicoll RA. Synapse-specific and developmentally regulated targeting of AMPA receptors by a family of MAGUK scaffolding proteins. Neuron. 2006; 52(2):307–320. [PubMed: 17046693]
16. Xu W, Schluter OM, Steiner P, Czervionke BL, Sabatini B, Malenka RC. Molecular dissociation of the role of PSD-95 in regulating synaptic strength and LTD. Neuron. 2008; 57(2):248–262. [PubMed: 18215622]
17. Opazo P, Sainlos M, Choquet D. Regulation of AMPA receptor surface diffusion by PSD-95 slots. Curr Opin Neurobiol. 2011; 22(3):453–460. [PubMed: 22051694]
18. Beique JC, Andrade R. PSD-95 regulates synaptic transmission and plasticity in rat cerebral cortex. J Physiol. 2003; 546(Pt 3):859–867. [PubMed: 12563010]
19. Colledge M, Snyder EM, Crozier RA, Soderling JA, Jin Y, Langeberg LK, et al. Ubiquitination regulates PSD-95 degradation and AMPA receptor surface expression. Neuron. 2003; 40(3):595–607. [PubMed: 14642282]
20. Sturgill JF, Steiner P, Czervionke BL, Sabatini BL. Distinct domains within PSD-95 mediate synaptic incorporation, stabilization, and activity-dependent trafficking. J Neurosci. 2009; 29(41): 12845–12854. [PubMed: 19828799]
21. Bhattacharyya S, Biou V, Xu W, Schluter O, Malenka RC. A critical role for PSD-95/AKAP interactions in endocytosis of synaptic AMPA receptors. Nat Neurosci. 2009; 12(2):172–181. [PubMed: 19169250]
22. Woods GF, Oh WC, Boudewyn LC, Mikula SK, Zito K. Loss of PSD-95 enrichment is not a prerequisite for spine retraction. J Neurosci. 2011; 31(34):12129–12138. [PubMed: 21865455]
23. Mao SC, Chang CH, Wu CC, Orejanera MJ, Manzoni OJ, Gean PW. Inhibition of spontaneous recovery of fear by mGluR5 after prolonged extinction training. PLoS One. 2013; 8(3):e59580. [PubMed: 23555716]
24. Mao SC, Lin HC, Gean PW. Augmentation of fear extinction by D-cycloserine is blocked by proteasome inhibitors. Neuropsychopharmacology. 2008; 33(13):3085–3095. [PubMed: 18368037]
25. Tsai NP, Wilkerson JR, Guo W, Maksimova MA, DeMartino GN, Cowan CW, et al. Multiple autism-linked genes mediate synapse elimination via proteasomal degradation of a synaptic scaffold PSD-95. Cell. 2012; 151(7):1581–1594. [PubMed: 23260144]
26. Rashid AJ, Cole CJ, Josselyn SA. Emerging roles for MEF2 transcription factors in memory. Genes Brain Behav. 2014
27. Migaud M, Charlesworth P, Dempster M, Webster LC, Watabe AM, Makhinson M, et al. Enhanced long-term potentiation and impaired learning in mice with mutant postsynaptic density-95 protein. Nature. 1998; 396(6710):433–439. [PubMed: 9853749]
28. Elkobi A, Ehrlich I, Belelovsky K, Barki-Harrington L, Rosenblum K. ERK-dependent PSD-95 induction in the gustatory cortex is necessary for taste learning, but not retrieval. Nat Neurosci. 2008; 11(10):1149–1151. [PubMed: 18776894]

29. Nithianantharajah J, Komiyama NH, McKechanie A, Johnstone M, Blackwood DH, Clair DS, et al. Synaptic scaffold evolution generated components of vertebrate cognitive complexity. Nat Neurosci. 2013; 16(1):16–24. [PubMed: 23201973]
30. Irvine EE, Drinkwater L, Radwanska K, Al-Qassab H, Smith MA, O'Brien M, et al. Insulin receptor substrate 2 is a negative regulator of memory formation. Learn Mem. 2012; 18(6):375–383. [PubMed: 21597043]
31. Li C, Brake WG, Romeo RD, Dunlop JC, Gordon M, Buzescu R, et al. Estrogen alters hippocampal dendritic spine shape and enhances synaptic protein immunoreactivity and spatial memory in female mice. Proc Natl Acad Sci U S A. 2004; 101(7):2185–2190. [PubMed: 14766964]
32. Liu F, Day M, Muniz LC, Bitran D, Arias R, Revilla-Sanchez R, et al. Activation of estrogen receptor-beta regulates hippocampal synaptic plasticity and improves memory. Nat Neurosci. 2008; 11(3):334–343. [PubMed: 18297067]
33. Camp MC, Feyder M, Ihne J, Palachick B, Hurd B, Karlsson RM, et al. A novel role for PSD-95 in mediating ethanol intoxication, drinking and place preference. Addict Biol. 2011; 16(3):428–439. [PubMed: 21309945]
34. Nagura H, Ishikawa Y, Kobayashi K, Takao K, Tanaka T, Nishikawa K, et al. Impaired synaptic clustering of postsynaptic density proteins and altered signal transmission in hippocampal neurons, and disrupted learning behavior in PDZ1 and PDZ2 ligand binding-deficient PSD-95 knockin mice. Mol Brain. 2012; 5:43. [PubMed: 23268962]
35. Yao WD, Gainetdinov RR, Arbuckle MI, Sotnikova TD, Cyr M, Beaulieu JM, et al. Identification of PSD-95 as a regulator of dopamine-mediated synaptic and behavioral plasticity. Neuron. 2004; 41(4):625–638. [PubMed: 14980210]
36. Feyder M, Karlsson RM, Mathur P, Lyman M, Bock R, Momenan R, et al. Association of mouse Dlg4 (PSD-95) gene deletion and human DLG4 gene variation with phenotypes relevant to autism spectrum disorders and Williams' syndrome. Am J Psychiatry. 2010; 167(12):1508–1517. [PubMed: 20952458]
37. Crusio WE, Goldowitz D, Holmes A, Wolfer D. Standards for the publication of mouse mutant studies. Genes Brain Behav. 2009; 8(1):1–4. [PubMed: 18778401]
38. Yang RJ, Mozhui K, Karlsson RM, Cameron HA, Williams RW, Holmes A. Variation in mouse basolateral amygdala volume is associated with differences in stress reactivity and fear learning. Neuropsychopharmacology. 2008; 33(11):2595–2604. [PubMed: 18185497]
39. Misane I, Tovote P, Meyer M, Spiess J, Ogren SO, Stiedl O. Time-dependent involvement of the dorsal hippocampus in trace fear conditioning in mice. Hippocampus. 2005; 15(4):418–426. [PubMed: 15669102]
40. Feyder M, Wiedholz L, Sprengel R, Holmes A. Impaired Associative Fear Learning in Mice with Complete Loss or Haploinsufficiency of AMPA GluR1 Receptors. Front Behav Neurosci. 2007; 1:4. [PubMed: 18958186]
41. Kinney JW, Starosta G, Holmes A, Wrenn CC, Yang RJ, Harris AP, et al. Deficits in trace cued fear conditioning in galanin-treated rats and galanin-overexpressing transgenic mice. Learn Mem. 2002; 9(4):178–190. [PubMed: 12177231]
42. Bouton ME. Context, ambiguity, and unlearning: sources of relapse after behavioral extinction. Biol Psychiatry. 2002; 52(10):976–986. [PubMed: 12437938]
43. Camp MC, Macpherson KP, Lederle L, Graybeal C, Gaburro S, Debrouse LM, et al. Genetic strain differences in learned fear inhibition associated with variation in neuroendocrine, autonomic, and amygdala dendritic phenotypes. Neuropsychopharmacology. 2012; 37(6):1534–1547. [PubMed: 22334122]
44. Frankland PW, O'Brien C, Ohno M, Kirkwood A, Silva AJ. Alpha-CaMKII-dependent plasticity in the cortex is required for permanent memory. Nature. 2001; 411(6835):309–313. [PubMed: 11357133]
45. Kim JJ, Fanselow MS. Modality-specific retrograde amnesia of fear. Science. 1992; 256(5057): 675–677. [PubMed: 1585183]

46. Whittle N, Hauschild M, Lubec G, Holmes A, Singewald N. Rescue of impaired fear extinction and normalization of cortico-amygdala circuit dysfunction in a genetic mouse model by dietary zinc restriction. J Neurosci. 2010; 30(41):13586–13596. [PubMed: 20943900]
47. Hefner K, Whittle N, Juhasz J, Norcross M, Karlsson RM, Saksida LM, et al. Impaired fear extinction learning and cortico-amygdala circuit abnormalities in a common genetic mouse strain. J Neurosci. 2008; 28(32):8074–8085. [PubMed: 18685032]
48. Holmes A, Fitzgerald PJ, Macpherson KP, Debrouse L, Colacicco G, Flynn SM, et al. Chronic alcohol remodels prefrontal neurons and disrupts NMDAR-mediated fear extinction encoding. Nat Neurosci. 2012; 15(10):1359–1361. [PubMed: 22941108]
49. Brigman JL, Daut RA, Wright T, Gunduz-Cinar O, Graybeal C, Davis MI, et al. GluN2B in corticostriatal circuits governs choice learning and choice shifting. Nat Neurosci. 2013; 16(8): 1101–1110. [PubMed: 23831965]
50. DePoy L, Daut R, Brigman JL, Macpherson K, Crowley N, Gunduz-Cinar O, et al. Chronic alcohol produces neuroadaptations to prime dorsal striatal learning. Proc Natl Acad Sci U S A. 2013; 110(36):14783–14788. [PubMed: 23959891]
51. Fitzgerald PJ, Whittle N, Flynn SM, Graybeal C, Pinard CR, Gunduz-Cinar O, et al. Prefrontal single-unit firing associated with deficient extinction in mice. Neurobiol Learn Mem. 2013
52. Burgos-Robles A, Vidal-Gonzalez I, Santini E, Quirk GJ. Consolidation of fear extinction requires NMDA receptor-dependent bursting in the ventromedial prefrontal cortex. Neuron. 2007; 53(6): 871–880. [PubMed: 17359921]
53. Boyden ES, Zhang F, Bamberg E, Nagel G, Deisseroth K. Millisecond-timescale, genetically targeted optical control of neural activity. Nat Neurosci. 2005; 8(9):1263–1268. [PubMed: 16116447]
54. McClure C, Cole KL, Wulff P, Klugmann M, Murray AJ. Production and titering of recombinant adeno-associated viral vectors. J Vis Exp. 2011; (57):e3348. [PubMed: 22143312]
55. During MJ, Young D, Baer K, Lawlor P, Klugmann M. Development and optimization of adeno-associated virus vector transfer into the central nervous system. Methods Mol Med. 2003; 76:221–236. [PubMed: 12526166]
56. Choi VW, Asokan A, Haberman RA, Samulski RJ. Production of recombinant adeno-associated viral vectors. Curr Protoc Hum Genet. 2007 Chapter 12: Unit 12 19.
57. Schluter OM, Xu W, Malenka RC. Alternative N-terminal domains of PSD-95 and SAP97 govern activity-dependent regulation of synaptic AMPA receptor function. Neuron. 2006; 51(1):99–111. [PubMed: 16815335]
58. Rodriguez A, Ehlenberger DB, Dickstein DL, Hof PR, Wearne SL. Automated three-dimensional detection and shape classification of dendritic spines from fluorescence microscopy images. PLoS ONE. 2008; 3(4):e1997. [PubMed: 18431482]
59. Horner CH, Arbuthnott E. Methods of estimation of spine density--are spines evenly distributed throughout the dendritic field? J Anat. 1991; 177:179–184. [PubMed: 1769892]
60. Raybuck JD, Lattal KM. Bridging the interval: Theory and neurobiology of trace conditioning. Behav Processes. 2013
61. Frankland PW, Ding HK, Takahashi E, Suzuki A, Kida S, Silva AJ. Stability of recent and remote contextual fear memory. Learn Mem. 2006; 13(4):451–457. [PubMed: 16882861]
62. Milekic MH, Alberini CM. Temporally graded requirement for protein synthesis following memory reactivation. Neuron. 2002; 36(3):521–525. [PubMed: 12408853]
63. Sacco T, Sacchetti B. Role of secondary sensory cortices in emotional memory storage and retrieval in rats. Science. 2010; 329(5992):649–656. [PubMed: 20689011]
64. Frankland PW, Bontempi B. The organization of recent and remote memories. Nat Rev Neurosci. 2005; 6(2):119–130. [PubMed: 15685217]
65. Takehara K, Kawahara S, Kirino Y. Time-dependent reorganization of the brain components underlying memory retention in trace eyeblink conditioning. J Neurosci. 2003; 23(30):9897–9905. [PubMed: 14586019]
66. Maviel T, Durkin TP, Menzaghi F, Bontempi B. Sites of neocortical reorganization critical for remote spatial memory. Science. 2004; 305(5680):96–99. [PubMed: 15232109]

67. Teixeira CM, Pomedli SR, Maei HR, Kee N, Frankland PW. Involvement of the anterior cingulate cortex in the expression of remote spatial memory. J Neurosci. 2006; 26(29):7555–7564. [PubMed: 16855083]
68. Ding HK, Teixeira CM, Frankland PW. Inactivation of the anterior cingulate cortex blocks expression of remote, but not recent, conditioned taste aversion memory. Learn Mem. 2008; 15(5): 290–293. [PubMed: 18441286]
69. Goshen I, Brodsky M, Prakash R, Wallace J, Gradinaru V, Ramakrishnan C, et al. Dynamics of retrieval strategies for remote memories. Cell. 2011; 147(3):678–689. [PubMed: 22019004]
70. Bontempi B, Laurent-Demir C, Destrade C, Jaffard R. Time-dependent reorganization of brain circuitry underlying long-term memory storage. Nature. 1999; 400(6745):671–675. [PubMed: 10458162]
71. Takashima A, Petersson KM, Rutters F, Tendolkar I, Jensen O, Zwarts MJ, et al. Declarative memory consolidation in humans: a prospective functional magnetic resonance imaging study. Proc Natl Acad Sci U S A. 2006; 103(3):756–761. [PubMed: 16407110]
72. Holahan MR, Routtenberg A. Post-translational synaptic protein modification as substrate for long-lasting, remote memory: an initial test. Hippocampus. 2007; 17(2):93–97. [PubMed: 17111412]
73. Quinn JJ, Ma QD, Tinsley MR, Koch C, Fanselow MS. Inverse temporal contributions of the dorsal hippocampus and medial prefrontal cortex to the expression of long-term fear memories. Learn Mem. 2008; 15(5):368–372. [PubMed: 18441294]
74. Koya E, Uejima JL, Wihbey KA, Bossert JM, Hope BT, Shaham Y. Role of ventral medial prefrontal cortex in incubation of cocaine craving. Neuropharmacology. 2009; 56(Suppl 1):177–185. [PubMed: 18565549]
75. Takehara-Nishiuchi K, McNaughton BL. Spontaneous changes of neocortical code for associative memory during consolidation. Science. 2008; 322(5903):960–963. [PubMed: 18988855]
76. Kim JJ, Clark RE, Thompson RF. Hippocampectomy impairs the memory of recently, but not remotely, acquired trace eyeblink conditioned responses. Behav Neurosci. 1995; 109(2):195–203. [PubMed: 7619310]
77. Frankland PW, Bontempi B, Talton LE, Kaczmarek L, Silva AJ. The involvement of the anterior cingulate cortex in remote contextual fear memory. Science. 2004; 304(5672):881–883. [PubMed: 15131309]
78. Euston DR, Gruber AJ, McNaughton BL. The role of medial prefrontal cortex in memory and decision making. Neuron. 2012; 76(6):1057–1070. [PubMed: 23259943]
79. Knapska E, Macias M, Mikosz M, Nowak A, Owczarek D, Wawrzyniak M, et al. Functional anatomy of neural circuits regulating fear and extinction. Proc Natl Acad Sci U S A. 2012; 109(42):17093–17098. [PubMed: 23027931]
80. Harvey CD, Svoboda K. Locally dynamic synaptic learning rules in pyramidal neuron dendrites. Nature. 2007; 450(7173):1195–1200. [PubMed: 18097401]
81. Steiner P, Higley MJ, Xu W, Czervionke BL, Malenka RC, Sabatini BL. Destabilization of the postsynaptic density by PSD-95 serine 73 phosphorylation inhibits spine growth and synaptic plasticity. Neuron. 2008; 60(5):788–802. [PubMed: 19081375]
82. Prange O, Murphy TH. Modular transport of postsynaptic density-95 clusters and association with stable spine precursors during early development of cortical neurons. J Neurosci. 2001; 21(23): 9325–9333. [PubMed: 11717366]
83. Meyer D, Bonhoeffer T, Scheuss V. Balance and stability of synaptic structures during synaptic plasticity. Neuron. 2014; 82(2):430–443. [PubMed: 24742464]
84. Vetere G, Restivo L, Cole CJ, Ross PJ, Ammassari-Teule M, Josselyn SA, et al. Spine growth in the anterior cingulate cortex is necessary for the consolidation of contextual fear memory. Proc Natl Acad Sci U S A. 2011; 108(20):8456–8460. [PubMed: 21531906]
85. Restivo L, Vetere G, Bontempi B, Ammassari-Teule M. The formation of recent and remote memory is associated with time-dependent formation of dendritic spines in the hippocampus and anterior cingulate cortex. J Neurosci. 2009; 29(25):8206–8214. [PubMed: 19553460]
86. Milad MR, Quirk GJ. Neurons in medial prefrontal cortex signal memory for fear extinction. Nature. 2002; 420(6911):70–74. [PubMed: 12422216]

87. Wilber AA, Walker AG, Southwood CJ, Farrell MR, Lin GL, Rebec GV, et al. Chronic stress alters neural activity in medial prefrontal cortex during retrieval of extinction. Neuroscience. 2011; 174:115–131. [PubMed: 21044660]

88. Sederberg PB, Kahana MJ, Howard MW, Donner EJ, Madsen JR. Theta and gamma oscillations during encoding predict subsequent recall. J Neurosci. 2003; 23(34):10809–10814. [PubMed: 14645473]

89. Headley DB, Weinberger NM. Fear conditioning enhances gamma oscillations and their entrainment of neurons representing the conditioned stimulus. J Neurosci. 2013; 33(13):5705–5717. [PubMed: 23536084]

90. Courtin J, Karalis N, Gonzalez-Campo C, Wurtz H, Herry C. Persistence of amygdala gamma oscillations during extinction learning predicts spontaneous fear recovery. Neurobiol Learn Mem. 2013

91. Lesting J, Narayanan RT, Kluge C, Sangha S, Seidenbecher T, Pape HC. Patterns of coupled theta activity in amygdala-hippocampal-prefrontal cortical circuits during fear extinction. PLoS One. 2011; 6(6):e21714. [PubMed: 21738775]

92. Courtin J, Chaudun F, Rozeske RR, Karalis N, Gonzalez-Campo C, Wurtz H, et al. Prefrontal parvalbumin interneurons shape neuronal activity to drive fear expression. Nature. 2014; 505(7481):92–96. [PubMed: 24256726]

93. Lesburgueres E, Gobbo OL, Alaux-Cantin S, Hambucken A, Trifilieff P, Bontempi B. Early tagging of cortical networks is required for the formation of enduring associative memory. Science. 2011; 331(6019):924–928. [PubMed: 21330548]

94. Zelikowsky M, Bissiere S, Fanselow MS. Contextual fear memories formed in the absence of the dorsal hippocampus decay across time. J Neurosci. 2012; 32(10):3393–3397. [PubMed: 22399761]

95. Poulos AM, Li V, Sterlace SS, Tokushige F, Ponnusamy R, Fanselow MS. Persistence of fear memory across time requires the basolateral amygdala complex. Proc Natl Acad Sci U S A. 2009; 106(28):11737–11741. [PubMed: 19567836]

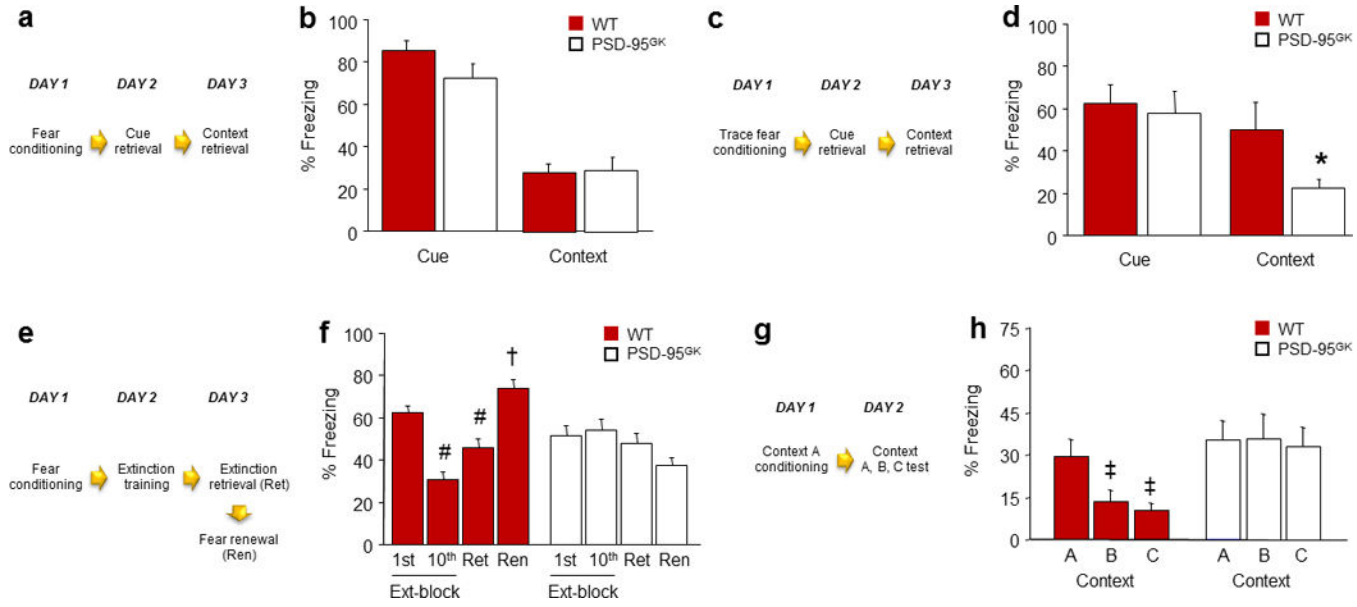

Figure 1. PSD-95 deletion does not affect retrieval of recent fear memories, but impairs their extinction and precision

(**a**) Schematic of experimental design for testing recent fear memory retrieval following delay conditioning. (**b**) Genotypes showed equivalent levels of freezing during cue and context retrieval (n=11–17). (**c**) Schematic of experimental design for testing recent fear memory retrieval following trace conditioning. (**d**) Following trace fear conditioning, genotypes showed similar cue fear retrieval, but PSD-95^{GK} mice froze significantly less than wild-type controls during context retrieval (n=8–10). (**e**) Schematic of experimental design for testing extinction of a recent fear memory. (**f**) WT controls, but not PSD-95^{GK} mice, decreased freezing from the first to the last extinction trial-block, and froze less during extinction retrieval as compared to the first trial-block of extinction training (n=11). (**g**) Schematic of experimental design for testing the precision of a recent contextual fear memory. (**h**) WT controls, but not PSD-95^{GK} mice, froze more to the conditioned context than either of two different contexts (n=13). Data are means ± SEM. **P*<.05 vs. WT/Context, #*P*<.05 vs. 1st Ext-block/WT, †*P*<.05 vs. Ren/WT, ‡*P*<.05 vs. Context A/WT

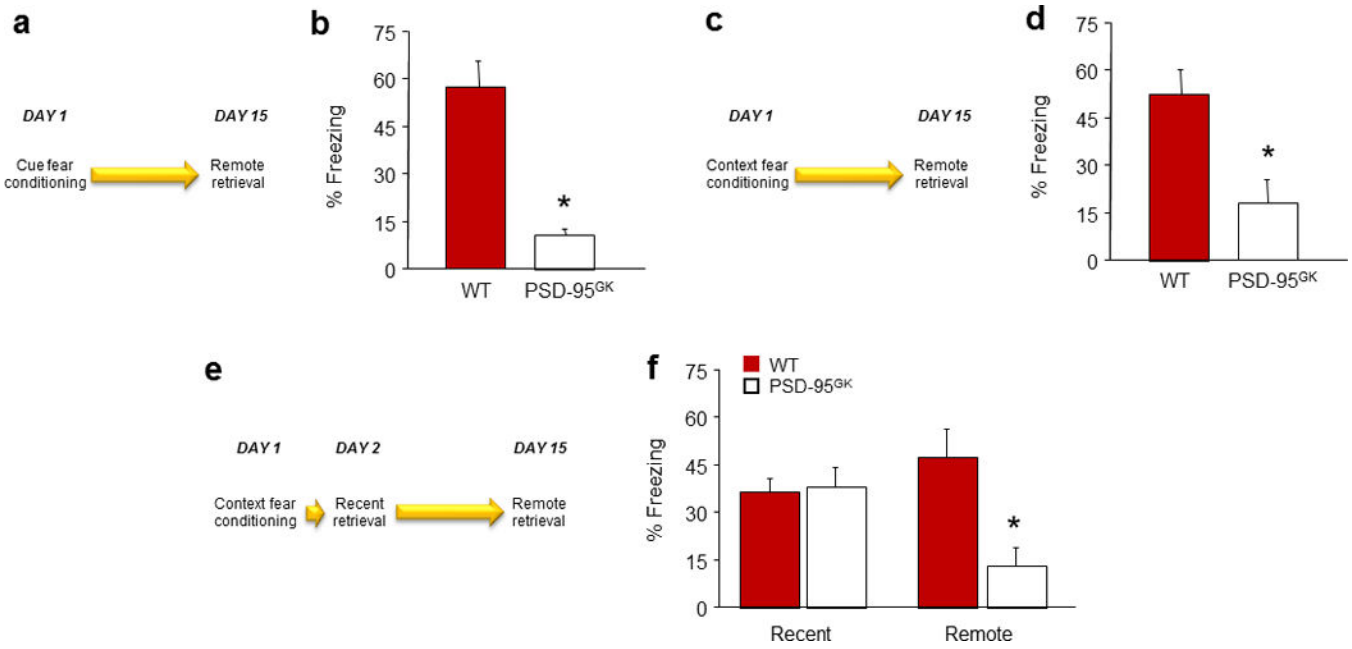

Figure 2. PSD-95 deletion impairs retrieval and stability of remote fear memories

(**a**) Schematic of experimental design for testing remote retrieval of a cued fear memory. (**b**) PSD-95^{GK} mice froze less than WT controls during remote fear memory retrieval (n=8–9). (**c**) Schematic of experimental design for testing the remote retrieval of a contextual fear memory. (**d**) PSD-95^{GK} mice froze less than WT controls during remote fear memory retrieval (n=9–10). (**e**) Schematic of experimental design for testing recent and remote retrieval of a contextual fear memory in the same mice. (**f**) PSD-95^{GK} mice froze less than WT controls during remote, but not recent, fear memory retrieval (n=8). Data are means ±SEM. *P<.05 vs. WT/same time point, †P<.05 vs. non-reactivated MUT

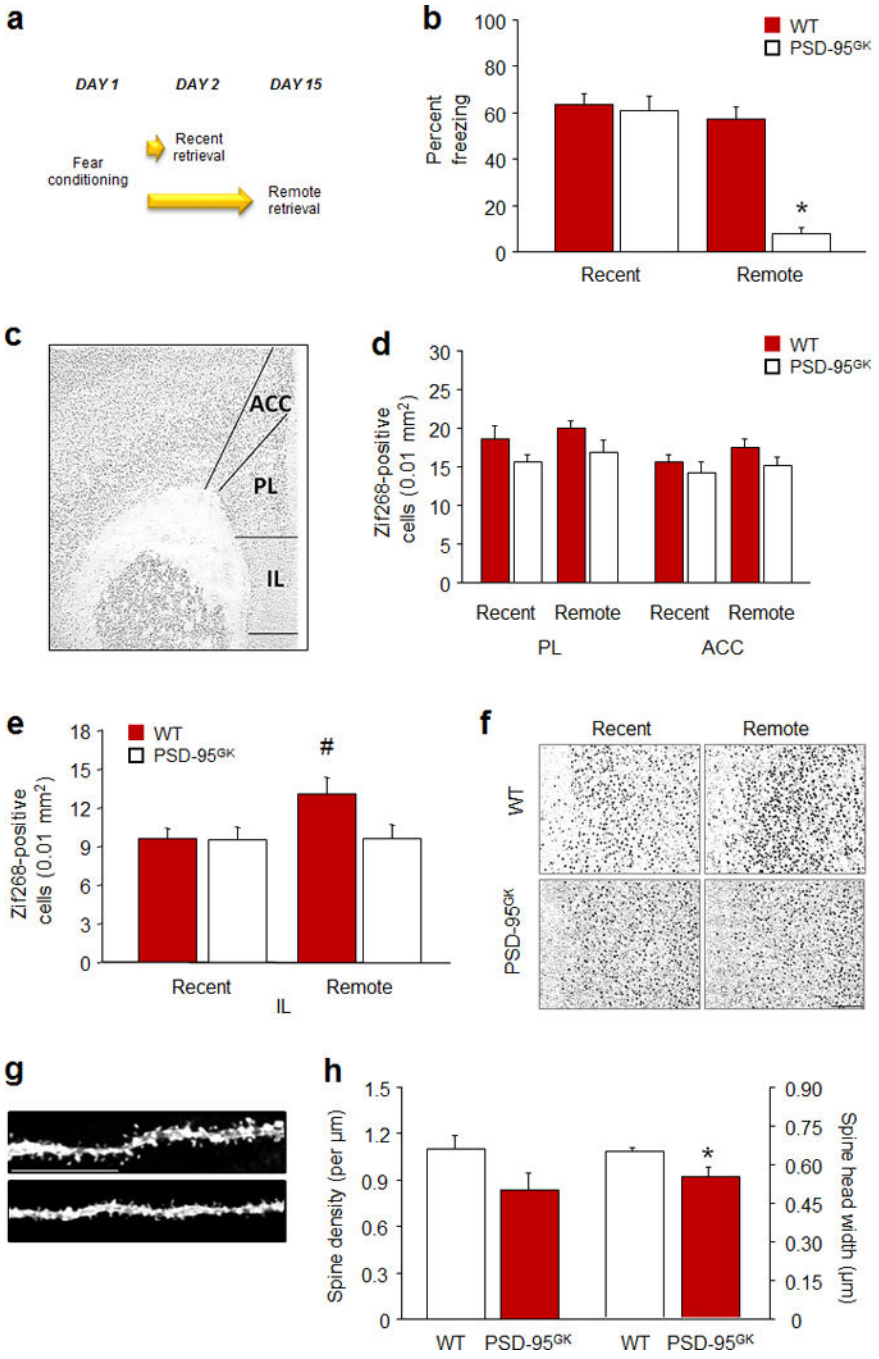

Figure 3. PSD-95 deletion disrupts activation of the infralimbic cortex during remote fear memory retrieval

(**a**) Schematic of experimental design for testing recent and remote retrieval of a cued fear memory. (**b**) PSD-95^{GK} mice froze less than WT controls during remote, but not recent, fear memory retrieval. (**c**) Representative Zif268-labelled coronal section showing the three prefrontal regions analyzed. (**d**) IEG analysis of prefrontal regions found no change in the number of Zif268-positive cells in either the anterior cingulate cortex (ACC, Cg1 subregion) or prelimbic cortex (PL), irrespective of memory age or genotype. (**e**) WT mice exhibited an

elevated number of Zif268-positive cells in the infralimbic cortex (IL) after remote, as compared to recent retrieval, while the number of cells did not increase in the PSD-95^{GK} mice. (**f**) Representative coronal sections showing Zif268-positive cells in the IL (scale bar= 150 μm). (**g**) Example images of dendritic spines in IL pyramidal neurons from a PSD-95 KO (top) and WT controls (bottom) (scale bar=15 μm). (**h**) PSD-95 KO mice had marginally lesser density and significantly lesser spine head width on IL pyramidal neurons, relative to WT controls (n=3 mice per group, n=7–12 cells per group). Data are means ±SEM. **P*<.05 vs. WT Remote or WT controls, #*P*<.05 vs. WT Recent

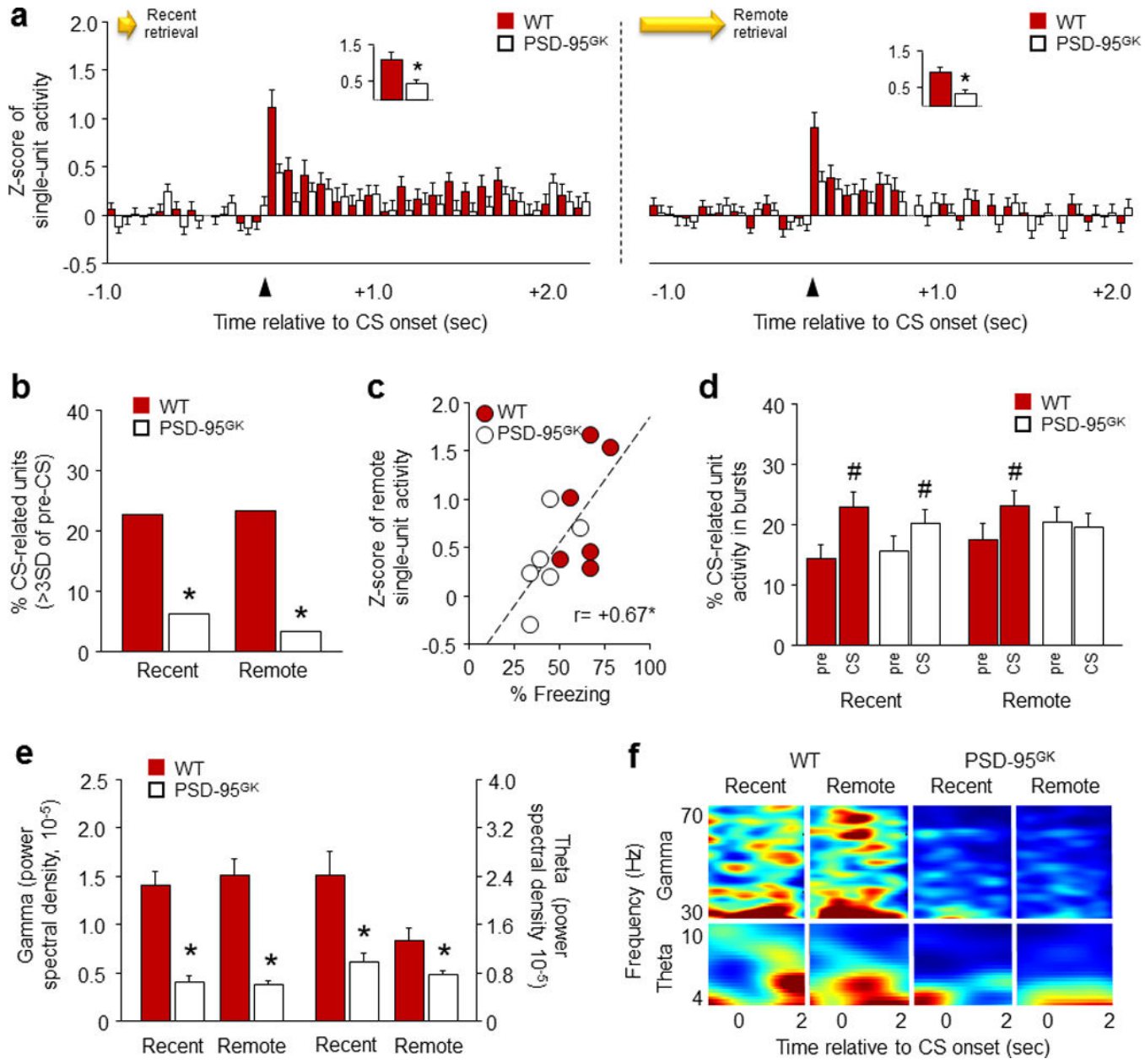

Figure 4. PSD-95 deletion disrupts CS-related single-unit activity in the infralimbic cortex during fear memory retrieval

(**a**) PSD-95^{GK} mice showed less CS-related IL single-unit activity than WT controls during recent (left panel) and remote (right panel) fear memory retrieval. Insets show first 100 millisecond timebins. (**b**) PSD-95^{GK} mice had fewer phasic CS-related IL single-units than WT controls during recent and remote retrieval. (**c**) IL single-unit activity correlated positively with freezing during remote retrieval. (**d**) IL single-unit burst activity increased during the CS in both genotypes during recent retrieval, but only in WT mice during remote retrieval. (**e**) PSD-95^{GK} mice showed lower gamma and theta oscillations than WT controls, on recent and remote retrievals. (**f**) Representative perievent spectrograms showing the gamma and theta frequency spectra around CS-onset. For gamma panels, darkest blue=0

mV^2*s and darkest red=$2e^{-5}$. For theta panels, darkest blue=0 and darkest red=$4e^{-4}$ mV^2*s. Data are means ±SEM. n=6 mice per genotype, n=74–87 single-units per genotype. *P<.05 vs. WT/same time point, #P<.05 vs. pre-CS/same genotype

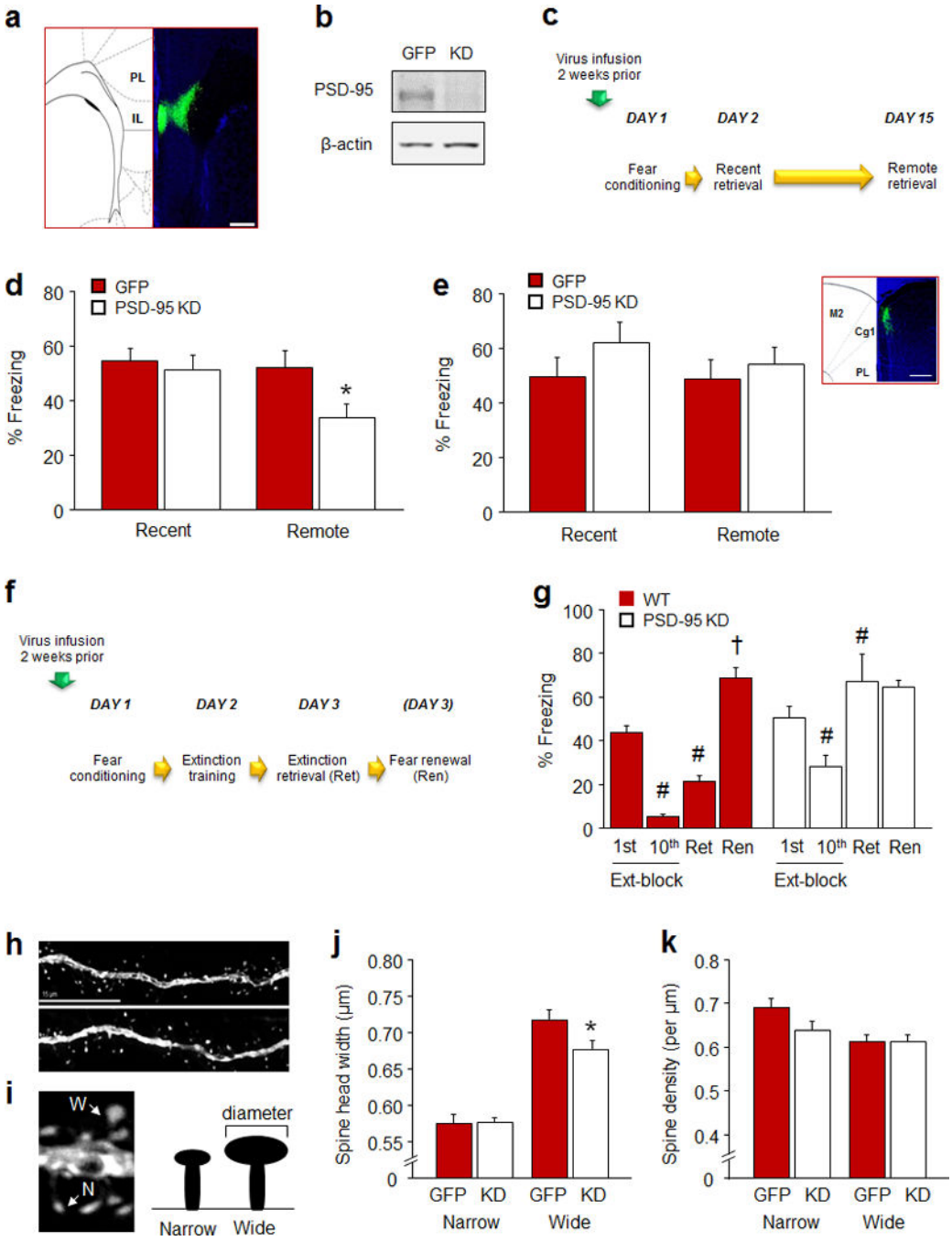

Figure 5. PSD-95 knockdown in infralimbic cortex impairs remote fear memory retrieval

(**a**) Example of green fluorescent protein (GFP) localization of the PSD-95 knockdown adenoassociated virus in the IL (scale bar=200 μm). (**b**) Example Western blots showing viral-induced knockdown of PSD-95 protein. (**c**) Schematic of experimental design for testing recent and remote retrieval of a cued fear memory. (**d**) IL PSD-95 KD mice showed less freezing than GFP-virus controls during remote, but not recent retrieval (n=12–17). (**e**) ACC PSD-95 KD mice showed similar freezing levels to GFP controls during recent and remote retrieval (n=9–11). Inset: example of GFP localization of the PSD-95 KD

adenoassociated virus in the Cg1 region of the ACC (scale bar=200 μm). (**f**) Schematic of experimental design for testing fear extinction. (**g**) IL PSD-95 KD mice decreased freezing from the first to the last extinction trial-block, but less so than GFP-virus controls. GFP-virus controls, but not IL PSD-95 KD mice, froze less during extinction retrieval as compared to the first trial-block of extinction training (n=7–9). (**h**) Example images of dendritic spines in IL pyramidal neurons from a PSD-95 KD (top) and GFP control (bottom) (scale bar=15 μm). (**i**) Examples and cartoon showing examples of narrow (N) and wide (W) subpopulations of dendritic spines. (**j,k**) PSD-95 KD decreased the spine head width, but not density, of relatively wide spines on IL pyramidal neurons, relative to GFP controls (n=7 mice per group, n=15–23 cells per group). Data are means ±SEM. **P*<.05 vs. PSD-95 KD/ same time point or spine subpopulation